MODELING AND SIMULATION OF E1784K MUTATION AND SODIUM IONIC CHANNEL DISEASES

Zhang Wen[1], *Yuan Yongfeng*[2], *Kong Shuhan*[2]

(1. School of Life Science, East China Normal University, Shanghai, 200062, P. R. China;
2. School of Computer Science and Technology, Harbin Institute of Technology, Harbin, 100051, P. R. China)

Abstract: In the clinical reports, the E1784K mutation in SCN5A is recognized as a phenotypic overlap between the long QT syndrome (LQT3) and the Brugada syndrome (BrS) in the characteristics of electrocardiograms (ECGs) since the mutation can influence sodium channel functions. However it is still unclear if the E1784K mutation-induced sodium ionic channel alterations account for the overlap at tissue level. Thsu, a detailed computational model is developed to underpin the functional impacts of the E1784K mutation on the action potential (AP), the effective refractory period (ERP) and the abnormal ECG. Simulation results suggest that the E1784K mutation-induced sodium channel alterations are insufficient to produce the phenotypic overlap between LQT3 and BrS, and the overlap may arise from the complicated effects of the E1784K mutation-induced changes in sodium channel currents with an increase of the transient outward current I_{To} or a decrease of the L-type calcium current I_{CaL}.

Key words: E1784K mutation; sodium ionic channel; long QT syndrome; Brugada syndrome

CLC number: TP391.9 **Document code**: A **Article ID**: 1005-1120(2011)04-0385-08

INTRODUCTION

E1784K is a mutation in SCN5A gene which is the control gene of sodium ionic channel. In clinical reports, electrocardiograms (ECGs) of patients with the E1784K mutation exhibit the characteristics of abnormal prolongation of QT interval and T segment elevation in the right precordial leads, which indicates a phenotypic overlap between long QT syndrome (LQT3) and Brugada syndrome (BrS). Makita et al[1] reported the E1784K mutation resulted in a shift of transient sodium current (I_{NaT}) inactivation curve in the hyperpolarising direction and an increase in density of late sodium current (I_{NaL}). However, it is still unclear whether the E1784K mutation-induced alternations in sodium channel functions are sufficient to illustrate the overlap between LQT3 and BrS. This problem is hard to validate by physiological experiment method[2-3]. Accordingly, in the present study, a computational model based on detailed experimental data is developed to investigate the problem as a hypothesis research method.

1 DEVELOPMENT OF COMPUTATIONAL MODEL

1.1 Altered kinetics of sodium ion channel under E1784K mutation condition

In the present study, the Ten Tusscher-Noble-Noble-Panfilov (TNNP) model which is the popular human ventricular cell computational model developed by Ten Tusscher et al[4] is used. Since the TNNP model does not include I_{NaL} model, a new ventricular I_{NaL} model is developed according to the I_{NaL} model[5] and the experimental data[6] on maximal conductance of I_{NaL} in three

Foundation items: Supported by the National Natural Science Foundation of China(61001167,61172149).

Received date: 2011-05-05; **revision received date**: 2011-07-08

E-mail: yongfeng.yuan@hit.edu.cn

types of canine ventricular cells, and then the model is incorporated into the TNNP cell computational model. Definition of the model is described as

$$\begin{cases} I_{\mathrm{NaL}} = G_{\mathrm{NaL}} m_{\mathrm{L}}^3 h_{\mathrm{L}} (V_{\mathrm{m}} - E_{\mathrm{Na}}) \\ \dfrac{\mathrm{d}m_L}{\mathrm{d}t} = \dfrac{m_{\mathrm{L}\infty} - m_{\mathrm{L}}}{\tau_{m_{\mathrm{L}}}} \\ m_{\mathrm{L}\infty} = \dfrac{\alpha_{m_{\mathrm{L}}}}{\alpha_{m_{\mathrm{L}}} + \beta_{m_{\mathrm{L}}}} \\ \tau_{m_{\mathrm{L}}} = \dfrac{1}{\alpha_{m_{\mathrm{L}}} + \beta_{m_{\mathrm{L}}}} \\ \alpha_{m_{\mathrm{L}}} = \dfrac{0.32 \times (V_{\mathrm{m}} + 47.13)}{1 - \exp(-0.1 \times (V_{\mathrm{m}} + 47.13))} \\ \beta_{m_{\mathrm{L}}} = 0.08 \times \exp \dfrac{-V_{\mathrm{m}}}{11.0} \\ \dfrac{\mathrm{d}h_{\mathrm{L}}}{\mathrm{d}t} = \dfrac{h_{\mathrm{L}\infty} - h_{\mathrm{L}}}{\tau_{h_{\mathrm{L}}}} \\ \tau_{h_{\mathrm{L}}} = 600 \\ h_{\mathrm{L}\infty} = \dfrac{1}{1 + \exp \dfrac{V_{\mathrm{m}} + 91}{6.1}} \end{cases} \quad (1)$$

where G_{NaL} is the maximal conductance of I_{NaL} channel and values of G_{NaL} for epicardial (EPI), midmyocaridal (M) and endocardial (ENDO) cell types are 0.006 5, 0.011 0 and 0.007 5 nS/pF respectively[6], m_{L} is the activation-gate variance, h_{L} the inactivation-gate variance, V_{m} the action potential(AP) of transmural membrane, E_{Na} the equilibrium potential of sodium channel currents and computed by extra-cellular sodium concentration $[\mathrm{Na}^+]_{\mathrm{o}}$ and intra-cellular sodium concentration $[\mathrm{Na}^+]_{\mathrm{i}}$ depending on the equation of Nernst (Eq. (2)).

$$E_{\mathrm{Na}} = \frac{RT}{F} \times \ln\left(\frac{[\mathrm{Na}^+]_{\mathrm{o}}}{[\mathrm{Na}^+]_{\mathrm{i}}}\right) \quad (2)$$

where R is the gas constant, F the Faraday constant and T the absolute temperature. $[\mathrm{Na}^+]_{\mathrm{o}}$ equals 140 mmol/L and $[\mathrm{Na}^+]_{\mathrm{i}}$ 5 mmol/L.

According to recent experimental data under the E1784K mutation condition, Makita et al[1] found that the activation and inactivation curves of I_{NaT} under the E1784K mutation condition were shifted to positive and negative directions compared with those under the control condition respectively.

The exponential regress equation (Eq. (3)) is used to simulate effects of the E1784K mutation on I_{NaT}.

$$y = \frac{a}{1 + \exp\left(\dfrac{x - x_{1/2}}{b}\right)^2} \quad (3)$$

where $x_{1/2}$ represents m (activation-gate variance) or h (inactivation-gate variance) in I_{NaT} kinetics of TNNP model. Depending on Makita's experimental observations[1], the values of $m_{1/2}$ are changed from −56.86 mV to −36.98 mV, and $h_{1/2}$ from −71.55 mV to −101.9 mV. The values of b are changed from −5.71 (control) to −7.67 (E1784K) for activation curve and from 5.97 (control) to 6.62 (E1784k) for inactivation curve respectively. Simulation results under both control and E1784K mutation conditions are shown in Fig. 1.

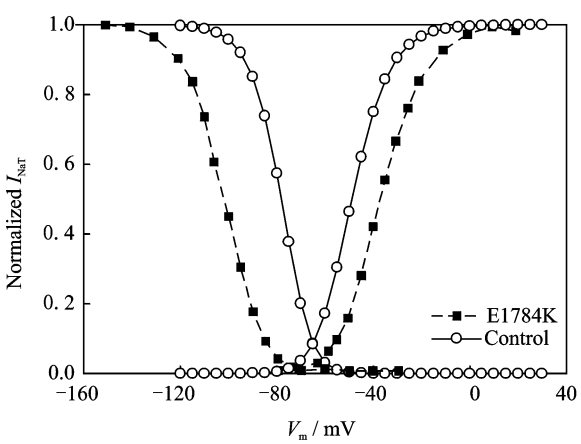

Fig. 1 Activation and inactivation curves of I_{NaT} under control and E1784K mutation conditions

1.2 Kinetics of calcium and potassium ion channels under BrS condition

The previous experimental studies[7-8] reported that the remarkable ST segment elevation in the right precordial ECG leads of BrS patients was associated with the depression of AP plateau from right ventricular outflow tract to ventricular epicardium, which was found to be related with an increase of the transient outward current I_{To} and a decrease of the L-type calcium current I_{CaL}. In order to simulate the effects of BrS-induced AP

changes of epicardium cell, the BrS model developed by Ref. [9] is used in this paper.

(1)Simulations of I_{To} kinetics changes under BrS condition

G_{To}, the maximum conductivity of I_{To}, is increased by 27% and activation curve of its activation-gate variance r is shifted from 20 mV to 2.5 mV.

(2)Simulations of I_{CaL} kinetics changes under BrS condition

G_{CaL}, the maximum conductivity of I_{CaL}, is reduced by 35%.

1.3 Ventricular tissue model

One-dimensional (1-D) model of transmural ventricular strand is composed of 100 computational cells (TNNP model) in series.

$$\frac{\partial V_m}{\partial t} = \frac{-I_{tot}}{C_m} + D \cdot \nabla V_m \qquad (4)$$

where t is the time, C_m the cell capacitance per unit surface area, D the diffusion coefficient which represents conduction speed, I_{tot} the total current across the membrane cell.

The length of each cell is 150 μm, while transmural human ventricular cell is about 50—100 μm. The length of transmural ventricular strand in stimulation is 15 mm whereas the real strand length of human is 4—14 mm. Following the results of Ref. [10], the length ratio of EPI, M and ENDO is 25 : 35 : 40. Except the EPI-M border, D is set to 0.054 mm²/ms. The conduction velocity of the simulated excitation wave is 0.48 m/s, and it belongs to the excitation conduction velocity scope of human heart chamber[10]. Due to the protective activities of ventricular tissue, there is a five-fold decrease in conduction velocity at the EPI-MIDDLE border. Accordingly, the value of D at this border is changed to 0.011 mm²/ms[6].

A 2-D transmural ventricular tissue sheet is modeled by expanding 1-D transmural strands. 1-D strand direction (x-direction) is recognized as transmural membrane direction and 800 strands are arranged along y-direction in parallel. Both spatial resolutions of x-and y-directions are 0.15 mm, so the volume of simulated ventricular tissue is 15×120 mm².

1.4 Computation of pseudo-ECG

Based on the 1-D strand model, a virtual electrode is set at 2 cm outside from the EPI end to simulate ECG (Fig. 2) using the method in Ref. [10]. According to source-field[11], the potential at virtual electrode is

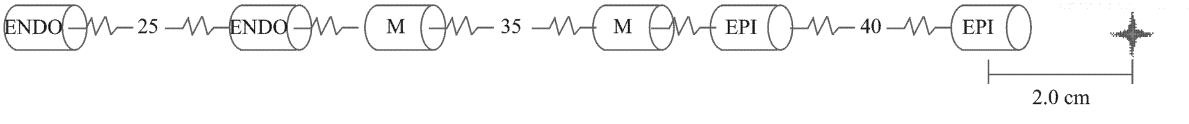

Fig. 2 Computational model of pseudo-ECG based on 1-D ventricular strand

$$\Phi_e = \frac{a^2\delta_i}{4\delta_e}\int(-\nabla V_m)\cdot\frac{1}{|x-x_0|}dx \qquad (5)$$

where Φ_e is the electric potential field of whole strand, δ_i and δ_e are the intra-and extra-cellular conductivities respectively, a is the radius of the cell, x the local site point of strand, x_0 the position of virtual electrode and $|x-x_0|$ the distance from the local site to the electrode. The potential at virtual electrode is computed as an integral of electric field consisted of all cells. Consistent with Ref. [9], the values of δ_i, δ_e and a are set to 0.000 74, 0.001 26 μs/cm and 0.001 1 cm.

2 SIMULATION RESULTS OF COMPUTATIONAL MODEL

2.1 Simulation results of altered sodium current under E1784K mutation condition

The current-voltage (I-V) curves of I_{NaT} obtained from simulation and experimental results are normalized and compared (Fig. 3). As illustrated, the curve shape and changing tendency of simulation data are nearly consistent with those of experimental data except the curve scope from −100 mV to −60 mV. In this range, the simula-

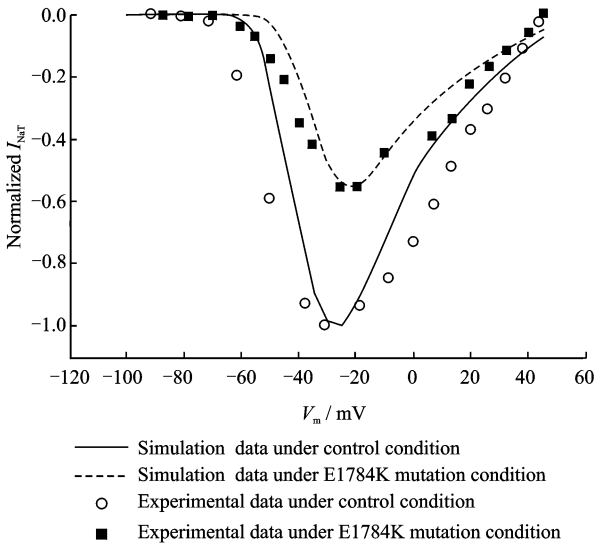

Fig. 3 Current-voltage (I-V) relations for I_{NaT} under control and E1784K mutation conditions

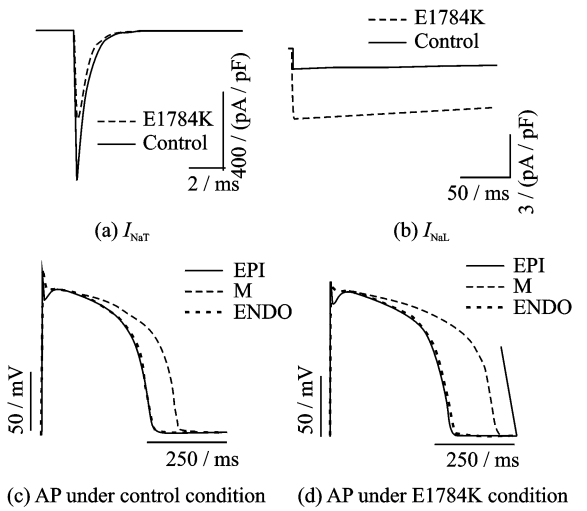

Fig. 4 Effects of I_{NaT} and I_{NaL} on AP

tion results are larger than experimental data. It is the main factor that the experimental conditions (such as temperature and instruments) for developed computational models are different from those in clone cell experiments. Furthermore, there are differences in physiological features between clone and original cells, for example, the I_{NaT} peak of clone cell is about five folds smaller than that of original cell. According to the shape and changing tendency of curves and physiological characters of I_{NaT}, the error between simulation and experimental results is within the acceptable range, which indicates the effectiveness of the above sodium ion channel model.

2.2 Comparison of action potentials

The effects of altered I_{NaT} and I_{NaL} under E1784K mutation condition on the cell AP are illustrated in Fig. 4. Compared with the control condition, the E1784K mutation condition results in a decrease in peak current density of I_{NaT} (Fig. 4(a)) and a persistent increase in I_{NaL} current (Fig. 4(b)). The altered I_{NaT} and I_{NaL} decrease the AP amplitude and prolong the AP duration (APD) of three ventricular cell types under E1784K mutation condition (Fig. 4(d)) in comparison with those under the control condition (Fig. 4(c)), and APDs are listed in Table 1.

Table 1 Effects of control and E1784K mutation conditions on APs of three ventricular cell types ms

APD_{90}	Control condition	E1784K condition
EPI	283.64	310.56
M	352.00	429.04
ENDO	285.30	316.68

2.3 Comparison of effective refractory period

As shown in Fig. 5, the computed ERPs under both control and E1784K mutation conditions are plotted against basic cycle length (BCL) for three cell types. Compared with the control condition, the E1784K mutation condition increases ERPs of three cell types in whole scope of BCL. As the augmented ERP of M cell is the largest, the heterogeneity among the different cell types is increased.

2.4 Simulation results of pseudo-ECGs

Simulation results of pseudo-ECGs in 1-D strand model under control and E1784K mutation conditions are illustrated in Fig. 6. Time-varying APs of each cell in 1-D strand are illustrated in the upper parts of the figure, and the different colors represent the different potentials. Time runs x-direction from left to right, while space of 1-D strand runs y-direction from the bottom (ENDO) to the top (EPI). In the bottom parts of the figure, time-varying pseudo-ECGs simulated by 1-D strand model are shown. Compared with

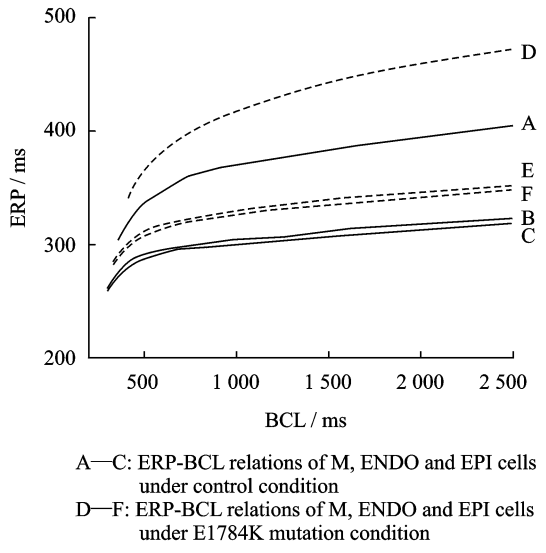

Fig. 5 ERP-BCL relations of three cell types under control and E1784K mutation conditions

the control condition (Fig. 6(a)), the pseudo-QT interval is prolonged and the amplitude and width of T-wave are increased under the E1784K mutation condition (Fig. 6(b)) because of the slow depolarization and repolarization of cells, the lengthened cell repolarization duration and the increased time difference of repolarization between cells induced by the E1784K mutation.

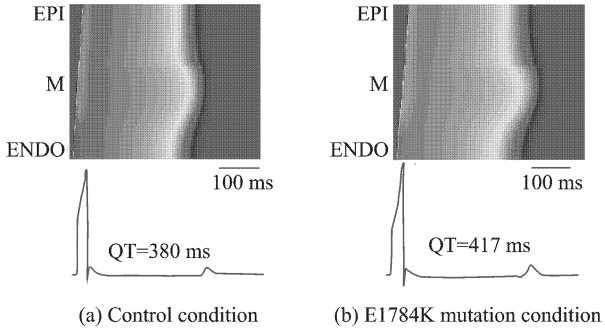

Fig. 6 Simulations of pseudo-ECGs under two conditions

3 ANALYSIS OF STIMULATION RESULTS

3.1 Analysis of physiological mechanism on stimulation results

The above simulation results indicate that the E1784K mutation decreases the peak current density of I_{NaT} but increases I_{NaL} current, APs and ERP. Furthermore, the dispersions of APs and ERP between cells are also enlarged. These changes result in the prolonged pseudo-QT interval and increase amplitude and width of T-wave. The prolonged QT interval and increased T-wave are typical ECG features of LQT3. But the ECG hallmark of BrS (elevated ST segment) has not been observed. Therefore, in this simulation study, the phenotypic overlap between LQT3 and BrS does not appear. These results suggest that the E1784K mutation-induced changes in sodium channel currents are insufficient to produce the phenotypic overlap between LQT3 and BrS. But why does the overlap appear in patients with the E1784K mutation?

The previous experimental research[12] found that the marked ST segment elevation in ECG of BrS was associated with the depression of the AP plateau in epicardium of right ventricular outflow, which was due to an increase of I_{To} current and a decrease of I_{CaL} current. This paper hypothesizes that function reconstructions of I_{To} and I_{CaL} currents under sodium channel dysfunctions caused by the E1784K mutation may be the major reason for producing the overlap between LQT3 and BrS. In order to validate the hypothesis, the two additional factors (increased I_{To} and decreased I_{CaL}) are reconsidered for the underlying mechanism of the E1784K mutation in this simulation.

Besides the effects of altered I_{To} and I_{CaL}, the altered kinetics of sodium current induced by the E1784K mutation also effects on APs of EPI cells and pseudo-ECGs. As shown in Fig. 7, under the E1784K mutation condition, there is not an obvious change on AP waveform of EPI cell except the markedly prolonged AP plateau. The QT-interval of pseudo-ECGs is prolonged and the amplitude and width of T-wave are increased. But the elevated ST segment is not observed.

APs and pseudo-ECGs of EPI cell are simulated via increasing I_{To} current using the methods in Section 1.2 (for EPI cell only, the I_{To} values of M and ENDO cells stay unchanged). Fig. 8 shows the waveforms of APs and pseudo-

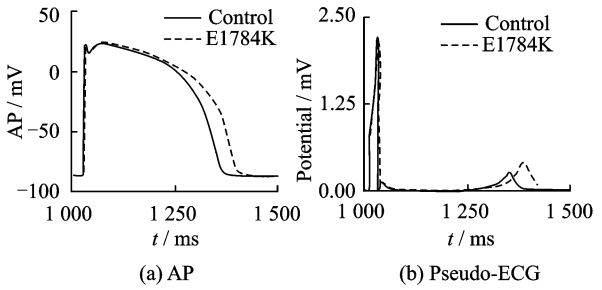

Fig. 7 APs and pseudo-ECGs of EPI cell under control and E1784K mutation conditions

ECGs under control, I_{To} (Brs Ⅰ) and "E1784K+I_{To}(Brs Ⅰ)" conditions. Compared with the control condition, a faster repolarization, lower AP plateau, shorter APD arise under the I_{To} condition. But they just show features of BrS Ⅰ in ECG (the domelike elevation of ST segment without the prolonged QT interval) and the features of LQT3 are not observed. The AP plateau and APDs are augmented under "E1784K+I_{To}" condition compared with those under I_{To} condition, but these two parameters are much shorter than those under control condition. And the ST segment are elevated like a dome (feature of BrS) while pseudo-QT interval are prolonged (feature of LQT3), thus exhibiting the overlap between LQT3 and BrS.

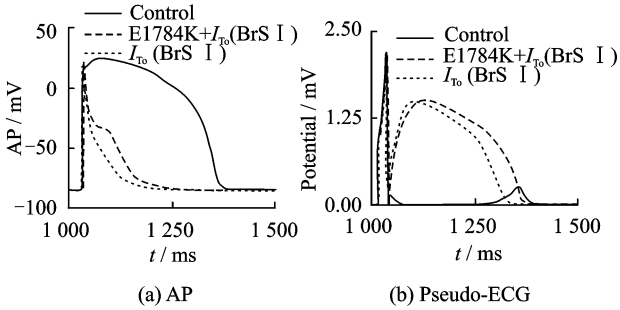

Fig. 8 APs and pseudo-ECGs of EPI cell under control, I_{To}(BrS Ⅰ) and "E1784K+I_{To}(BrS Ⅰ)" conditions

APs and pseudo-ECGs of EPI cell are simulated via decreasing I_{CaL} current using the stimulation methods of BrS (I_{CaL} values of M and ENDO cells stay unchanged)[12]. Fig. 9 shows the waveforms of APs and pseudo-ECGs under control, decreased I_{CaL} (BrS Ⅱ) and "E1784K+I_{CaL} (BrS Ⅱ)" conditions, respectively. Compared with the control condition, there are a faster repolarization, lower AP plateau, shorter APD and elevated ST segment like a saddle after simulation of decreased I_{CaL}. But the prolonged QT interval is not observed. The features of BrS Ⅱ in ECG just appear under the "E1784K+I_{CaL}" condition, and there is a mild decrease in AP plateau but an increase in APD compared with those under control condition. Also under this condition, features of both LQT3 ECG (prolonged pseudo-QT interval) and BrS ECG (elevated ST segment in pseudo-ECGs) are observed, thus indicating the overlap between LQT3 and BrS.

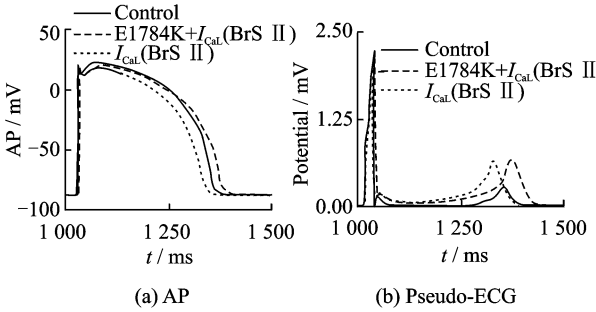

Fig. 9 APs and pseudo-ECGs of EPI cell under control, I_{CaL} (BrS Ⅱ) and "E1784K+I_{CaL} (BrS Ⅱ)" conditions

3.2 Simulation Limitations

There are some limitations in the model: (1) The TNNP model has not included I_{NaL}, and there are only canine experimental data of I_{NaL}; (2)Due to the lack of experimental data about the reconstruction of I_{To} or I_{CaL} induced by altered sodium channel, we directly use the results in Ref. [9] and assume that the altered sodium channel induced by the E1784K mutation results in an increase of I_{To} and a decrease of I_{CaL}. Accordingly, the precise reconstruction mechanisms of I_{To} or I_{CaL} induced by altered sodium channel cannot be obtained from the present work. However, these limitations do not influence the principal conclusions of this paper, that is, the E1784K mutation-induced sodium channel changes is insufficient to produce the phenotypic overlap between

LQT3 and BrS, which may arise from a combined action of the mutation-induced changes in sodium channel currents and possible increased I_{To} or decreased I_{CaL} as seen in BrS.

4 CONCLUSION

To study the problem wether the E1784K mutation-induced sodium ionic channel alterations account for the overlap at tissue level, the simulation is implemented by the detailed computational model incorporated with experimental data in Ref. [1]. The simulation results indicate that E1784K mutation-induced sodium channel alterations can explain increased APD and prolonged QT interval in the clinical ECGs, but cannot account for elevated ST segment observed in ECGs of patients with the E1784K gene mutation. The additional stimulations of I_{To} and I_{CaL} show features of BrS Ⅰ and BrS Ⅱ without the LQT3 features respectively. The phenotypic overlap between LQT3 and BrS phenomenon is only reproduced by the integration of I_{Na} and I_{To} or I_{Na} and I_{CaL}. Hence, the underlying cause of the phenotypic overlap of LQT3 and BrS may be a combined action of the E1784K mutation-induced changes in sodium channel currents with an increase of I_{To} or a decrease of I_{CaL}. In conclusion, the principal result in this paper suggests that the E1784K mutation-induced sodium current dysfunction is insufficient to produce the phenotypic overlap between LQT3 and BrS. The experimental study or clinical therapy about the E1784K mutation should not just concentrate on the direct cause of the E1784K regulating-sodium channel but consider the complicated reconstruction effects of other channels such as $I_{To}$and I_{CaL}currents caused by the E1784K mutation.

References:

[1] Makita N, Behr E, Shimizu W, et al. The E1784K mutation in SCN5A is associated with mixed clinical phenotype of type 3 long QT syndrome [J]. The Journal of Clinical Investigation, 2008, 118(6): 2219-2229.

[2] Zimmer T, Surber R. SCN5A channelopathies—An update on mutations and mechanisms [J]. Progress in Biophysics and Molecular Biology, 2008, 98(2/3): 120-136.

[3] Kapplinger J D, Tester D J, Alders M, et al. An international compendium of mutations in the SCN5A-encoded cardiac sodium channel in patients referred for Brugada syndrome genetic testing [J]. Heart Rhythm, 2010, 7(1): 33-46.

[4] Ten Tusscher K H, Noble D, Noble P J, et al. A model for human ventricular tissue [J]. American Journal of Physiology-Heart and Circulatory Physiology, 2004, 286(4): H1573-1589.

[5] Xia L, Zhang Y, Zhang H, et al. Simulation of Brugada syndrome using cellular and three-dimensional whole-heart modeling approaches [J]. Physiological Measurement, 2006, 27(11): 1125-1142.

[6] Yan G X, Shimizu W, Antzelevitch C. Characteristics and distribution of M cells in arterially perfused canine left ventricular wedge preparations [J]. Circulation, 1998, 98: 1921-1927.

[7] Yan G X, Antzelevitch C. Cellular basis for the Brugada syndrome and other mechanisms of arrhythmogenesis associated with ST-segment elevation [J]. Circulation, 1999, 100: 1660-1666.

[8] Fish J M, Antzelevitch C. Cellular mechanism and arrhythmogenic potential of T-wave alternans in the Brugada syndrome [J]. Journal of Cardiovascular Electrophysiology, 2008, 19: 301-308.

[9] Ten Tusscher K H, Panfilov A V. Cell model for efficient simulation of wave propagation in human ventricular tissue under normal and pathological conditions [J]. Physics in Medicine and Biology, 2006, 51(23): 6141-6156.

[10] Zhang H, Hancox J C. In silico study of action potential and QT interval shortening due to loss of inactivation of the cardiac rapid delayed rectifier potassium current [J]. Biochemical and Biophysical Research Communications, 2004, 322(2): 693-699.

[11] Jaakko M, Robert P. Bioelectromagnetism: Principles and Applications of Bioelectric and Biomagnetic Fields [M]. New York: Oxford University Press, 1995: 148-158.

[12] Satoshi N, Kengo F K, Hiroshi M, et al. Longer repolarization in the epicardium at the right ventricular outflow tract causes type 1 electrocardiogram in patients with Brugada syndrome [J]. Journal of the American College of Cardiology, 2008, 51(12): 1154-1161.

E1784K 基因变异与钠离子通道病建模与仿真

张 雯[1] 袁永峰[2] 孔姝涵[2]

(1. 华东师范大学生命科学学院,上海, 200062,中国;
2. 哈尔滨工业大学计算机科学与技术学院,哈尔滨,150001,中国)

摘要:临床报道发现SCN5A 上的一个位点突变E1784K 基因变异会导致同时出现长QT 间期III 型综合征和Brugada 综合征的特征。E1784K 基因变异引起钠离子通道功能改变,但无法确定钠离子通道功能的改变是否能够解释LQT3 和BrS 交叠现象。为分析该问题,建立了详细的计算模型,从动作电位、有效不应期和伪心电图三方面进行仿真。仿真结果表明E1784K 基因突变导致钠离子通道改变不能直接解释LQT3 和BrS 心电图特征交叠现象,而间接引起的I_{To}或者I_{CaL}重构可以解释该现象。

关键词:E1784K 基因变异;钠离子通道;长QT 间期III 型综合征;Brugada 综合征

中图分类号:TP391.9

(Executive editor: Zhang Huangqun)

基金项目:国家自然科学基金(61001167,61172149)资助项目。